Suppressing the non-Gaussian statistics of Renewable Power from Wind and Solar

M. Anvari, G. Lohmann, M. Reza Rahimi Tabar, M. Wächter, P. Milan, D. Heinemann, and Joachim Peinke
Institute of Physics and ForWind, Carl von Ossietzky University, 26111 Oldenburg, Germany

E. Lorenz
Department of Energy and Semiconductor Research, Institute of Physics, Carl von Ossietzky University, 26111 Oldenburg, Germany

The power from wind and solar exhibits a nonlinear flickering variability, which typically occurs at time scales of a few seconds. We show that high-frequency monitoring of such renewable powers enables us to detect a transition, controlled by the field size, where the output power qualitatively changes its behaviour from a flickering type to a diffusive stochastic behaviour. We find that the intermittency and strong non-Gaussian behavior in cumulative power of the total field, even for a country-wide installation still survives for both renewable sources. To overcome the short time intermittency, we introduce a time-delayed feedback method for power output of wind farm and solar field that can change further the underlying stochastic process and suppress their strong non-gaussian fluctuations.

I. INTRODUCTION

The renewable sources and their share in electricity production has been increased constantly, driven by mainly energy policies, markets and environmental issues. Among the renewable energy sources the use of wind power and photovoltaics (PV) has a priority in the future. For instance in the European Union, these renewable energies shall account for about 20 % of the gross final energy consumption by 2020 and 60 % by 2050 [1]. These renewable sources have new specific stochastic behaviour which is likely can cause instability in power grids provided that are simply added to the existing grids by replacing conventional technologies such as hydro, gas, coal, and nuclear power plants [2,3]. Therefore a revision of traditional power grids, which were not designed to have a large number of decentralised intermittent energy sources [1, 3, 4, 5, 6, 7], becomes necessary.

The typical time scales for the alternations of wind power and solar energy is in the range of seconds to minutes. Considering the strongly stochastic behaviour in these short time scales, the investigations of grid dynamics and its stability become more complex [3, 8, 9, 10, 11, 12, 13, 14, 15]. In particular, as pointed out in the following, a new demand for a fast managing system scoping with these short time power fluctuations will emerge [16, 17].

Nowadays, electronic converters are commonly used to connect intermittent solar and wind power generators to the grid at specified grid frequency of 50/60 Hz, thus the generators are almost decoupled from the grid load (they possess some synthetic inertia). These almost decoupled wind and solar power systems progressively replace the traditional synchronous generators in power plants. The inertia of fast rotating generators in normal power plants is used as an automatic power reserve - the so-called primary reserve - to match fast changes in the power demand. This is done simply by speeding up or slowing down the generator, changing the grid frequency by typically few mHz around the specified value. In the future electric grids, that will be driven by an increasing share of renewable sources, the capacity of primary reserve from traditional power plants will strongly decrease. Therefore, in this context, it is of great importance to have a precise characterization and understanding of the short-time fluctuations of wind and solar installations in the time range of seconds.

Next we aim to characterise the fluctuations of wind power and solar energy and analyse their short time intermittency and non-guassian statistics and finally propose a method to suppress such events. The results presented here are derived from measured data from operating wind turbines and from continuous solar irradiance in several regions around the world (the United States, Germany, Ireland, Algeria-Sahara and Spain). The sampling rates range from 0.001Hz to 1Hz. The data sets used are presented in appendix A, table I. The analysed time series $X(t)$ are scaled wind power $P(t)/P_r$, where P_r is the rated power, and the scaled clear sky index $G(t)/G_{clearsky}$, where $G(t)$ is the solar irradiance. The time series of clear sky index have positive values and their maxima are around unity [18, 19, 20]. The details are presented in appendices B, C, D, E, F and G.

II. INTERMITTENT, NON-GAUSSIAN BEHAVIOUR OF SOLAR IRRADIANCE AND WIND POWER INCREMENTS FLUCTUATIONS

The wind power and solar irradiance time series are strongly intermittent and possess irregular alternations. Wind turbulence is responsible for the short time scale intermittency of wind power [3, 21, 22, 23, 24, 25, 26], see supplementary information. For photovoltaics the dynamics of the clouds and their size distributions are the origin of its intermittent and jumpy behaviour [25, 27, 28, 29, 30, 31, 32, 33, 34, 35, 36, 37, 38, 39]. Due to the clouds dynamics one expects that the solar irradiance and clear sky index, possess a flickering type structure (on-off type behaviour), making solar power more intermittent than wind power which shows smaller jumps. Intermittent behaviour can be quantified through increments statistics, i.e. $X_\tau = X(t+\tau) - X(t)$, see appendix H, [40, 41, 42, 43, 44]. Extreme values of increments characterise large fluctuations over the time τ and are seen as gusts for wind or, respectively, as strong jumps due to clouds dynamics for solar. These increments X_τ are also of practical use, which they describe the expected relative change in the power production, seen from the present state $X(t)$ [26]. The probability of these events are quantified by increment probability density functions (PDF) $P(X_\tau)$. We use normalized increments X_τ/σ_τ, where σ_τ is the standard deviation of X_τ, so that normalized increment PDFs can be compared with a Gaussian distribution with standard deviation unity.

Increment PDFs are shown in the (Figs. 1a, 1b) (for time lags $\tau = 1, 10, 1000$ secs) for solar irradiance and wind power time series. They depart largely from the normal (Gaussian) distribution, as they possess exponential-like fat tails for both the single wind turbine and the single solar sensor as well for wind farm and solar field. These tails extend to extreme values, corresponding to a higher-than-normal probability to record an "extreme event". If common Gaussian-distributed processes are used for a grid model, these extreme events will not be taken into account in their stability analysis. For instance, a 20 $\sigma_{\tau=1s}$ fluctuation is observed on average once a month for wind power, but based on a Gaussian process it would be expected only once every 3 million years. The increment PDFs also show that solar irradiance has much more frequent extreme events than the wind power, as shown in the inset of (Fig. 1a).

For instance, the probability to observe our $20\sigma_{\tau=1s}$ fluctuation in solar irradiance, is one order of magnitudes higher than for wind power and for same rated powers. This means that ten, $20\sigma_{\tau=1s}$ events are likely to happen within one month. Thus extreme events in the solar irradiance fluctuations are much more frequent in short time scales and their integration into the power grid needs more detailed elaborations. We find similar non-Gaussian behaviour for Increment PDFs of solar irradiance in several regions around the world, including Sahara, Spain and Germany, (Fig. 2) see also the appendix B about the relation of solar irradiance and PV power.

The lag-dependence of the flatness and skewness as the measures for the non-Gaussianity of the increment PDFs, are shown in (Fig.3a, Fig.3b) for the wind velocity as well as for the wind and solar power. The non-Gaussian behaviour remains for the cumulative power output of a wind farm and solar field, even for country-wide installations, such as in Ireland and Germany (see (Fig. 4, Fig. 5. Fig. 6)) [45]. This is a direct consequence of the long-range correlations of wind velocity and cloud size distributions that are ~ 600 km and ~ 2100 km, respectively [46,47]. Therefore, the central-limit theorem does not apply and the cumulative power output increments does not converge to the expected Gaussian statistics and remains non-Gaussian.

In (Figs. 7a,7b,7e), we plot the effective potential of the dynamic $U_{eff}(Z)$ for the measured irradiance in the single sensor and the field, in Hawaii (data set a) and Germany (data set b), respectively. In the both cases, the effective potential for single sensor is asymmetric with a double-well structure. This demonstrates the existence of a metastable point (tipping point) for the single sensors at $Z = 0.8$ and $Z = 0.65$ for solar data set a and b, respectively. In the inset of (Fig. 7a), the flickering behaviour of the measured irradiance fluctuations between two minima is shown, see also supplementary movie S1. The first minimum in the effective potential corresponds to a "cloudy" state, while the second minimum is related to a "clear sky" or "sunny" state. The minima of higher depth will have a higher occupation probability. In (Fig. 7b), it is shown that the increase of the number of sensors (the size of the solar field) leads to shallower potentials, and the barrier between the two minima approaches zero, causing a slowing down in the dynamics. As a consequence of this slowing down, the system has a longer memory and its dynamics are characterised by a small jump rate and a higher correlation time scale. A similar trend exists for the data from the German solar field, as shown in (Fig. 7e) but the field size is not large enough to detect the transition. This means that the critical field size is not a universal length scale and depends on the climate of the area under investigation. The important observation is that larger fields have smoother clear sky index fluctuations. A rapid change of dynamics remains for small field sizes, that result in a more intermittent dynamics. This observation is important for the integration of solar energy into existing power grids. The radius of the potential well is directly related to the correlation time scale, which tends towards infinity as bifurcation is approached [50]. The empirical reconstruction of the basins of attraction (as seen from the effective potential) indicates that the resilience of the states varies with the field's size. Resilience is defined as the width of the basin of attraction around a stable state and diminishes towards the bifurcation point. In (Fig. 7f), a two-dimensional contour plot of the effective potential $U_{eff}(Z)$ is plotted for various field sizes (estimated as the square root of the field area). It shows how the potential flattens as the spanned area increases, for clear-sky index $Z < 1$. (Figs. 7c,7d) show the correlation between the clear sky index at two subsequent times (t and $t + 1$ secs) for single sensor and solar field, respectively. In a similar way, in (Fig. 8), we plotted the $U_{eff}(P)$ for wind park with a varying number of wind turbines and identify a similar transition as has been found in the solar field.

III. SUPPRESSING THE NON-GAUSSIAN STATISTICS

The output power from wind farm and solar fields vary on a time scale of seconds to minutes, up to several hours. Their variations are not completely predictable and may have positive or negative correlation with peak demand. Although the present detailed discussions of high frequency power fluctuations of renewable energies have not been reported so far, there is a common discussion on methods to handle the more volatile power system by means of i) reducing correlation of variation with spatial dispersion of sources and diverse portfolio of sources (e.g. solar + wind power); ii) using the "back up" dispatchable sources that can be ramped up and down for balancing the load and generated power; iii) energy storage, such as compressed air storage system, flywheels, superconductors, and batteries (although the cost of such advanced energy storage technologies is often put forward as their main limitation); iv) trade in electricity across countries, and finally v) improvements in transmission capacity, flexibility and grid management (including smart grid technologies) to have resilient power grids. The power electronics technology provides power controllability and can, in principal, limit at any time the power production very quickly. For negative increments (ramp down) the energy storage capacity can help to have a smooth decreasing of power [53, 54, 55]. It is not only the electronics technology, but also the interplay with the intrinsic dynamics of the various power systems that determines the feasibility under cost and efficiency constraints.

There have been many studies performed on intelligent solutions to overcome the intermittency of wind and solar power [56, 57]. For instance, short- and long-terms forecasting of power fluctuations can provide important information for energy management systems [3, 58, 59, 60, 61, 62].

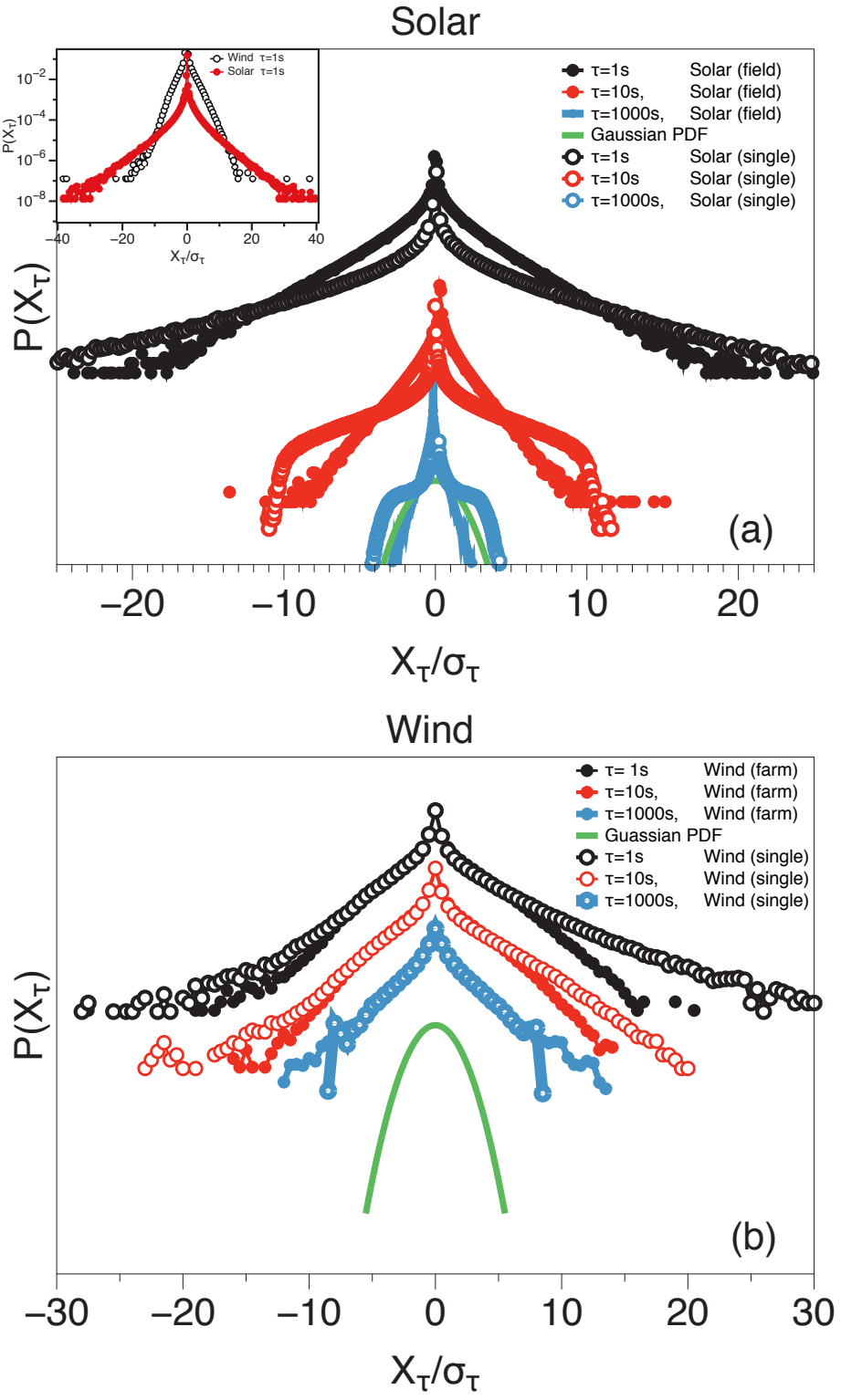

FIG. 1. Probability distribution functions (PDF) of increment statistics, $P(X_\tau)$ for solar and wind power fluctuations. a) Continuous deformation of the increment PDFs for time lags $\tau = 1, 10, 1000$ sec in log-linear scale, for the solar irradiance fluctuations of a single sensor and the whole field (for data measured in Hawaii). The PDFs are shifted in the vertical direction for convenience of presentation and X_τs are measured in units of their standard deviation σ_τ. b) Same figure for the increment PDFs of one wind turbine and a wind farm power for the same time lags. A Gaussian PDF with unit variance is plotted for comparison. In the inset of Fig. (a), we compare the increment PDFs of wind and solar power time series having a similar rated power with time lag 1sec. Extreme events up to about 20 $\sigma_{\tau=1}$ are recorded in the wind power, and up to about 40 σ_τ for solar irradiance in this time lag. It shows, for instance, the probability of observing a 20 σ_τ fluctuation of solar irradiance in 1sec is one order of magnitude higher than that of the wind power. This means that solar irradiance has much more frequent extreme events. The dot size is chosen in the order of the statistical error.

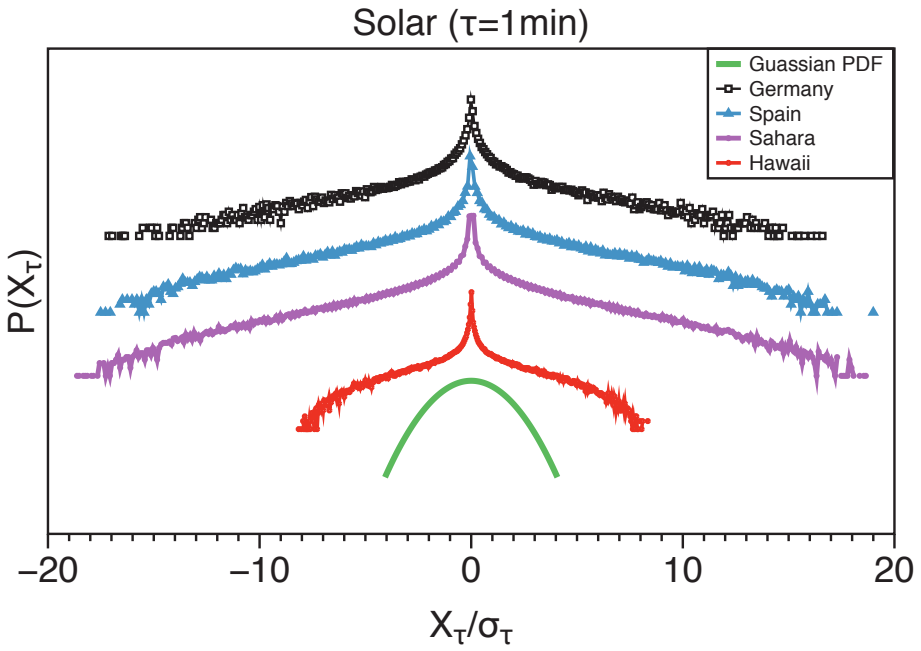

FIG. 2. Probability distribution functions (PDF) of increment statistics, $P(X_\tau)$ for (one minute averaged) solar irradiance in several regions around the world (Hawaii, Sahara, Spain, Germany) for time lag=1min. The PDFs are shifted in the vertical direction for convenience of presentation and X_τs are measured in units of their standard deviation σ_τ. Extreme events up to about 20 $\sigma_{\tau=1min}$ are recorded.

As another "smart" solution, we propose a time-delayed feedback method for suppressing the short-term intermittency of power output of wind and solar fields [63, 64]. This method enables the assessment of operation strategies for power systems and can be a complementary method for energy storage and two state-of-the-art strategies, ramp-rate control and moving average [54, 55, 65, 66, 67, 68, 69, 70, 71, 72, 73, 74, 75, 76, 77, 78].

In time-delayed feedback method the variation of total output of wind farm and solar fields depend on their past state (here, 2-5 seconds). By choosing the amplification coefficient α, as a fraction of power that can be saved by reservoirs and delay lag T in the feedback loop, we can reduce the short-term extreme events.

Consider time dependent (spatially-averaged) cumulative power of wind farm or solar field $P^*(t) = N^{-1}\sum_{i=1}^{N} p_i(t)$, where $p_i(t)$s are the power output of i-th intermittent sources (wind turbine or solar cell) and N is the number of sites (wind turbines or solar plates). For each time step, let save an α fraction of power in each site (and inject the saved power after T seconds), so that (1-α) fraction of power is imported to power grid directly. Then, the power output is:

$$p_i(t)^{new} = (1-\alpha)p_i(t) + \epsilon P^*(t-T) \tag{1}$$

where, in general, $\epsilon \leq \alpha$. For the power conserved-model the coupling ϵ is equal to α. The cumulative power output $\sum_i^N p_i(t)^{new}$ depends on the delay lag T and amplification α. Their optimal values can be determined from minimization of, for example, increment flatness. For our analyzed data we found that the optimal time delay-lag is about $2-5$ seconds, and the increment flatness decreases strongly with increasing the coefficients α. For instance, with $T = 5$ secs, the flatness of increments decreases from 12.6 to 6.5 for wind farm (see Fig. 9). The probability density of power increments of a wind park and solar field is plotted in Fig. 9c and 9d. The suppressing of strong non-Gaussian statistics is evident.

IV. CONCLUDING REMARKS

By increasing the shares of renewable energies, there has been more attention paid to system effects relating to the interaction of intermittent renewables with present dispatchable technologies. From a structural view point, power grids are complex networks which, due to economic factors, often run near their operational limits. In power grids the extreme events, such as power outages, exhibit many features of complex systems in which many interdependent

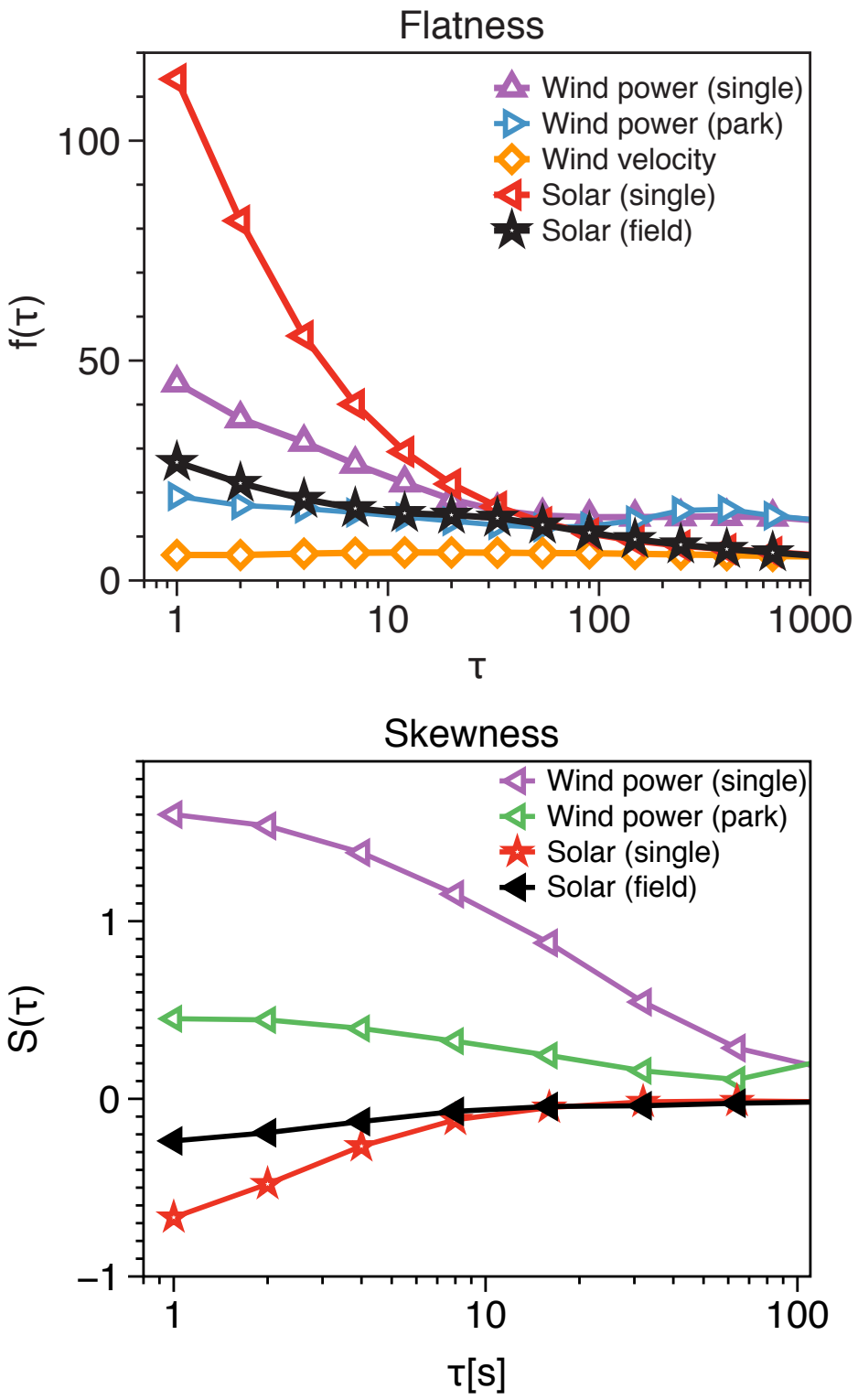

FIG. 3. a) The lag-dependence of the flatness $f(\tau) = S_4(\tau)/S_2(\tau)^2$, (where $S_{2k} = \langle (X(t+\tau) - X(t))^{2k} \rangle$) for solar irradiance, wind power and wind velocity fluctuations. They deviate strongly from the value 3, specially in short time scale, that corresponds to a Gaussian distribution. This shows that the power output of both renewable sources is more intermittent than wind velocity, which has an intermittent, turbulent character by itself. For the time lag $\tau = 1$ sec, the flatness reaches values $30-120$ for solar irradiance data, $20-40$ for wind power data and 6 for wind velocity. This means that wind turbines transfer wind intermittency to the grid, and even increase it. b) The lag-dependence of the skewness $S(\tau) = S_3(\tau)/S_2(\tau)^{3/2}$, for solar irradiance and wind power fluctuations. They deviate strongly from the zero, in short time scale, that corresponds to a symmetric distribution. Wind power and solar irradiance have positive and negative skewness, respectively, in short time scales.

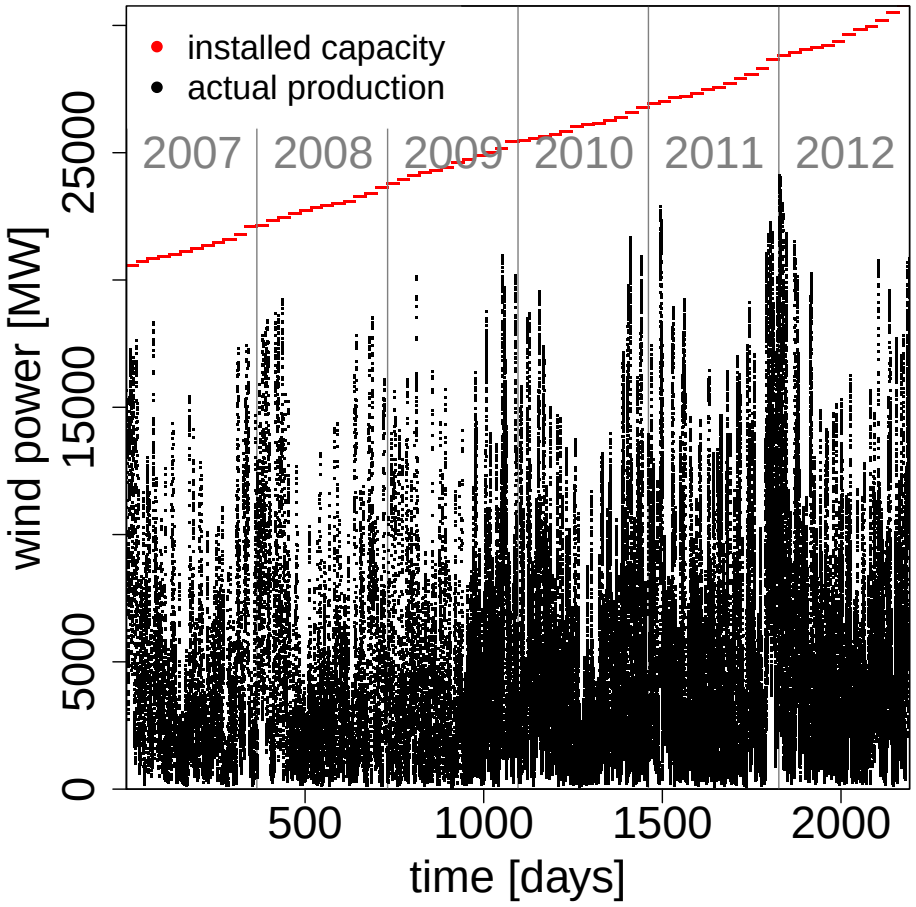

FIG. 4. Total wind power output in Germany, showing a strongly intermittent behaviour. The red line shows the installed capacity.

components lead to organized as well as irregular features. Power grid can be viewed as a system of systems where each system is comprised of a diverse set of passive and active components. They are not isolated systems and must be understood in terms of interactions among different components in the grid. Nowadays with increasing the share of intermittent renewable energy sources the complex network of power grids in practice, interacts with another important complex network i.e. climate/weather system. Understanding the constituents of interaction of two complex systems (power grid & climate/weather system) and simulating their collective presence will allow for the efficient design of resilient power grid with desirable emergent properties.

The complexity of weather dynamics leads to small scale non-Gaussian statistics in the power production from renewable sources, such as wind and solar [51, 52, 79, 80]. Here we provide strong evidence that these sources exhibit multiple types of variability and nonlinearity in the time scales of seconds and minutes and are strongly intermittent with irregular alternations. As a consequence of this increased complexity in the power dynamics, any central management of the grid is likely to become more and more difficult as the shares in renewable energies increases. Therefore the probability of having the grid instabilities will increase, which may result in more frequent occurrences of extreme events like cascading failures resulting in large blackouts. Any strategy under discussion, like upgrading the existing power grid, the formation of virtual power plants combining different power sources, introducing new storage capacities, introducing intelligent "smart grid" concepts, etc., will further increase the complexity of the existing systems and has to be based on the detailed knowledge of the dynamics of these renewable energies. Investigations of *power grids* stability in the presence of *stochastic renewable sources*, including their extreme events, provide a new emerging field of research which is a new combination of these so far disconnected fields of work [3, 4, 16, 81, 82, 83, 84, 85, 86, 87].

We propose an approach for analysing the intermittent behaviour of wind and solar power, using the increment

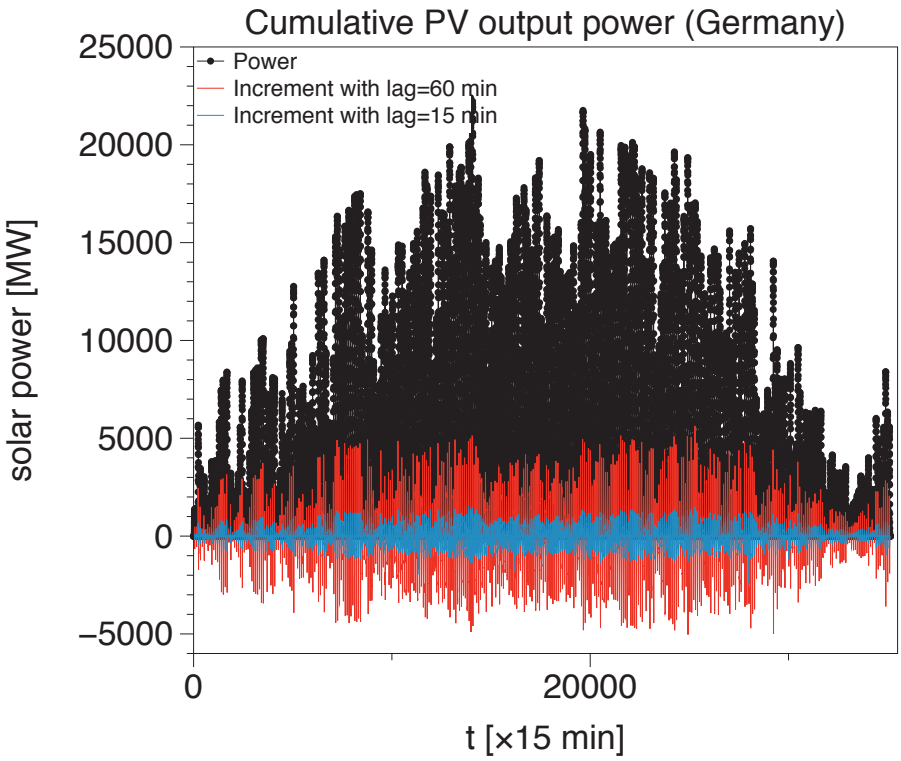

FIG. 5. Total solar power output and its increments in time lags 15min and 1h in Germany for year 2012, showing a strongly intermittent behaviour. The installed capacity is about $\sim 30GW$.

statistics and effective potential of dynamics, which will help pave the way to the design and robust evaluation of the stability of power grids. Our findings suggest that high-frequency monitoring of such renewable powers enables us to detect a transition, controlled by the field size, where the output power qualitatively changes its behaviour from a flickering type to a diffusive or persistent stochastic behaviour.

The flickering power output will demand more sophisticated methods to compensate for their on-off type behaviour and necessitates quick action (of order of seconds for solar and few minutes for wind power) in response to observed power variability [88]. Finally, we show that using a time delayed feedback method in the management of intermittent renewable sources will strongly suppresses the non-gaussian statistics. This method enables the assessment of operation strategies for power systems and can be a complementary method for energy storage and two state-of-the-art strategies, ramp-rate control and moving average to grid managements in time spans below 5 seconds, since for higher times, conventional solutions are known. Our proposed delayed feedback approach to mitigate power fluctuation could be even more effective if more than one energy storage system be used, each one with different time lag.

We believe such statistical analysis yield important information that must be included in the guidelines to guarantee an optimal design of resilient power grids. The challenge will be to fine tune the intelligent management tools, as well as technological possibilities, to achieve a stable and low cost power system that can handle efficiently the intermittent renewable sources of power.

Acknowledgments: The Lower Saxony research network 'Smart Nord' acknowledges the support of the Lower Saxony Ministry of Science and Culture through the 'Niedersächsisches Vorab' grant programme (grant ZN 2764/ZN 2896). We acknowledge also the National Renewable Energy Laboratory in the United States for providing the data in Hawaii. BSRN data was kindly made available by the World Radiation Monitoring Center (WRMC) and we particularly acknowledge Mohamed Mimouni and Xabier Olano, Managers of BSRN stations of Tamanrasset (Algeria) and Cener (Spain), respectively. We also acknowledge Deutsche Windtechnik AG Bremen for providing us with wind turbine data. We would like to thank, K. Aihara, L. von Bremen, J. Davoudi, O. Kamps, H. Kantz, L. Kocarev, J. Kurths, P. Lind, N. Nafari, J. F. Pinton, S. Rahvar, P. Rinn, M. Sahimi, K. Schmietendorf, M. Sonnenschein and K. R. Sreenivasan for important comments and discussions.

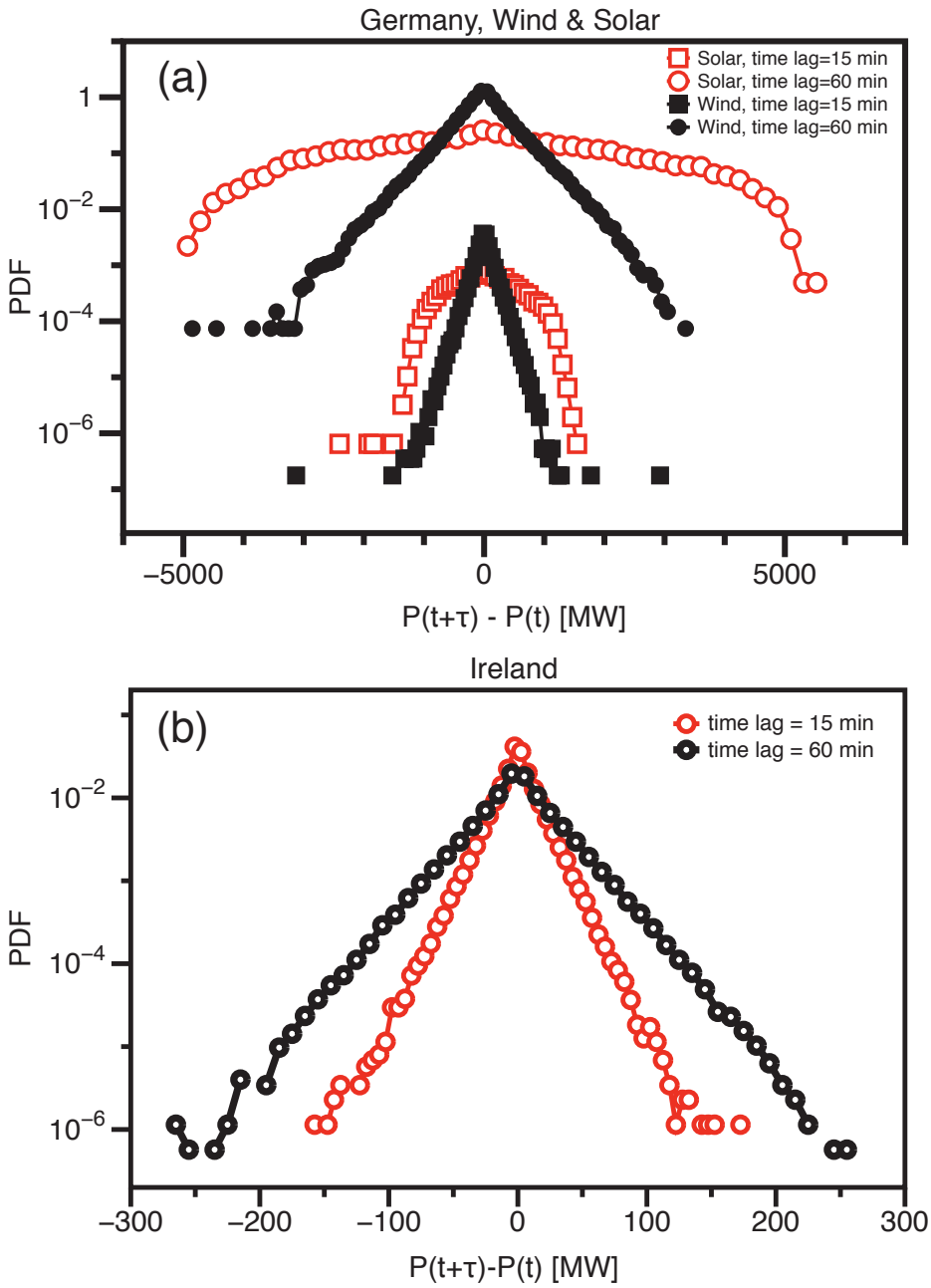

FIG. 6. Deformation of the increments PDFs for time lags $\tau = 15, 60$ min in log-linear scale, for wind and solar powers (a) in Germany (with a rated power $\sim 30GW$) and for wind power (b) in Ireland (with a rated power $\sim 1GW$). Extreme events up to about $\pm 2000MW$ ($\pm 150MW$) and $\pm 4000MW$ ($\pm 300MW$) are recorded in time lags 15 min and 60 min, in Germany (Ireland), respectively. In time lag 60 min the extreme events up to $\pm 6000MW$ are recorded in cumulative PV output of in Germany, with rated power about $\sim 30GW$. It shows that the probability of observing a ± 4000 MW fluctuation of solar power in 60 min is two orders of magnitude higher than that of the wind power for almost same rated power. We note that the solar variation from hour to hour/regional scale, the largest contributions are due to the deterministic course of irradiance, where sun has largest angular velocity. There were three classes of cloud situations: clear sky (no clouds for large regions and time scales of days), overcast (more or less homogenous cloud cover over larger regions) and finally variable clouds where large fluctuations are expected.

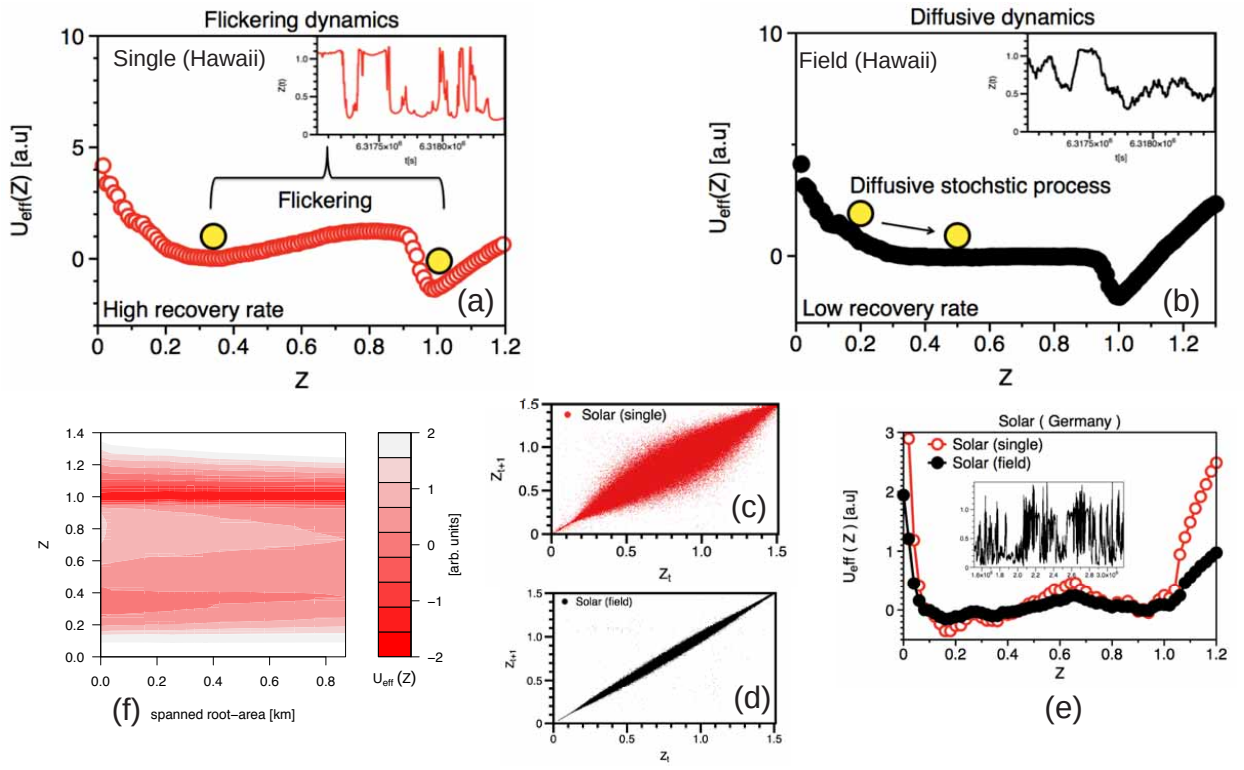

FIG. 7. Illustration of the transition and critical slowing down when increasing the field size from a single sensor (a) to the entire field (b). Panels show characteristic changes in stochastic dynamics of clear sky index as the dynamics approaches a tipping point or catastrophic bifurcation. As shown in the inset (a) the time series for a single sensor has a flickering behaviour, while for the field in the inset of (b), it has a diffusive stochastic behaviour (without strong jumps). The time series in the insets are belong to the Hawaii. (c) The resulting dynamics for single sensor is characterized by a moderate correlation between the clear sky index at two subsequent times. (d) for the entire filed the resulting dynamics are characterized by a stronger correlation between subsequent states. For the entire solar field, the double well structure of the effective potential becomes more shallow and thus the barrier height ($|U_{eff}(Z_{minimum}) - U_{eff}(Z_{maximum})|$) decreased. (b) shows that when increasing the number of sensors (or area of field) the first minimum (corresponds to the cloudy state) of clear sky index disappears. For the solar irradiance data in Hawaii a behavioural transition occurs for a critical field size of about $\sim 1 \times 1 km^2$. For the data in Germany (e) similar trend exists but the field is not large enough to detect this transition. (f) A two-dimensional contour plot of the effective potential $U_{eff}(Z)$ of clear sky index is plotted as a function of the field size (estimated as the square root of the field area). The data for this plot were measured in Hawaii.

V. APPENDICES

A. Data description

Table I provides a description for the wind energy data sets as well as the data for wind velocity and solar irradiance. The number of data points collected is provided as well as the duration and sampling frequency of the measurement campaign. The wind farm 1 has 12 wind turbines spread over a rectangular area of roughly $4 \times 4\ km^2$.

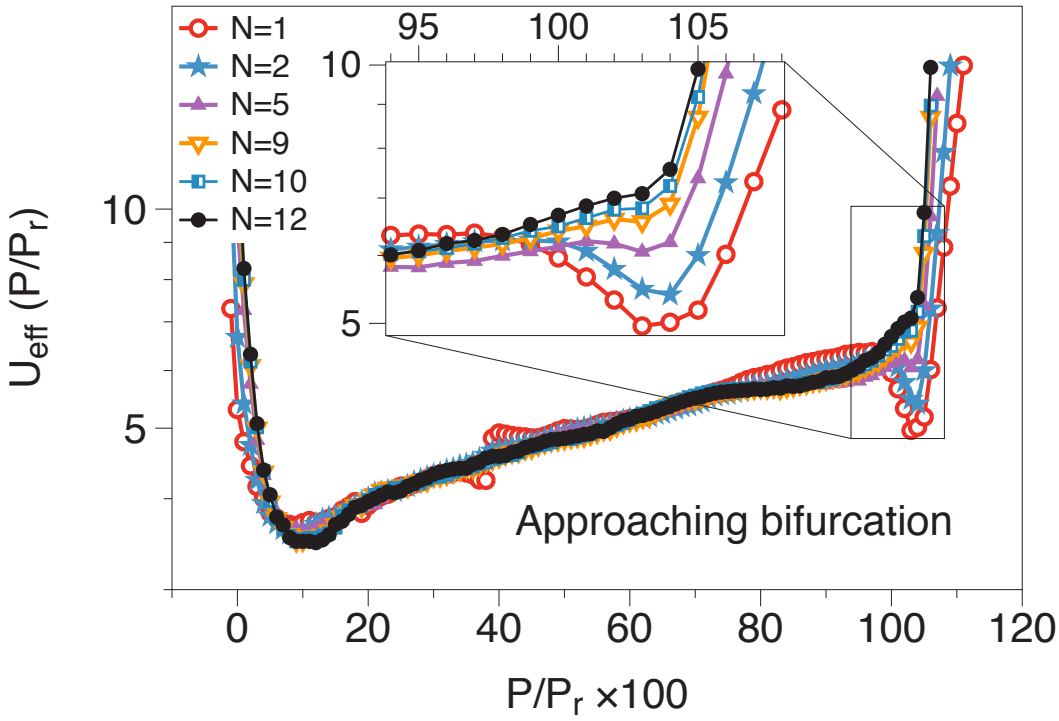

FIG. 8. Effective potential of the wind park $U_{eff}(P/P_r)$ and its dependence on the number of wind turbines. The valleys or potential wells represent stable attractors. It reveals two distinct attractors, at about 10 % and 103 % of the rated power for the single wind turbine. When increasing the number of wind turbines in the park, the double-well structure changes to a potential with a single minimum at $\sim 10\%$. The critical number of turbines for the behavioural transition is about $n_c \simeq 10$ turbines (with an area $\sim 4km^2$). The tipping point is located at $P/P_r \simeq 100\%$. The radius of the potential well is directly related to the system response time to small perturbations, which tends towards infinity as the bifurcation is approached, that is, the system has more inertia in response to perturbations (critical slowing down). Larger fluctuations are also expected as the bifurcation is approached.

TABLE I

dataset	rated power	data points	measurement/total	frequency	wind speed
wind farm 1	$\sim$ 25 MW	$15.3 \cdot 10^6$	$\sim$ 8 months	1 Hz	u
solar irradiance, Germany	–	$12 \cdot 10^6$	~16 months	1 Hz	–
solar irradiance, Hawaii	–	$14 \cdot 10^6$	~12 months	1 Hz	–
solar irradiance, Sahara	–	$3.7 \cdot 10^6$	~86 months	1/60 Hz	–
solar irradiance, Spain	–	$1.3 \cdot 10^6$	~31 months	1/60 Hz	–
wind farm Ireland	$\sim$ 1000 MW	$\sim 10^6$	$\sim$ 10 years	1/15 min^{-1}	–
wind farm Germany	$\sim$ 30 GW	$\sim 2 \cdot 10^5$	$\sim$ 6 years	1/15 min^{-1}	–
solar field Germany	$\sim$ 30 GW	$\sim$ 17000	$\sim$ 1 years	1/15 min^{-1}	–

B. Wind energy conversions

Industrial-sized wind turbines operate close to the ground, in a strongly turbulent layer of the atmosphere. High-frequency measurements of atmospheric wind speed reveal turbulent statistics close to those observed in ideal three-dimensional turbulent flows at short temporal scales. Such statistics are closely related to the concept of a turbulent cascade first introduced by Richardson, where the energy of large eddies *cascades* down from the large eddy structures towards smaller structures. Such three-dimensional flows exhibit intermittency, defined here as the nature of the flow

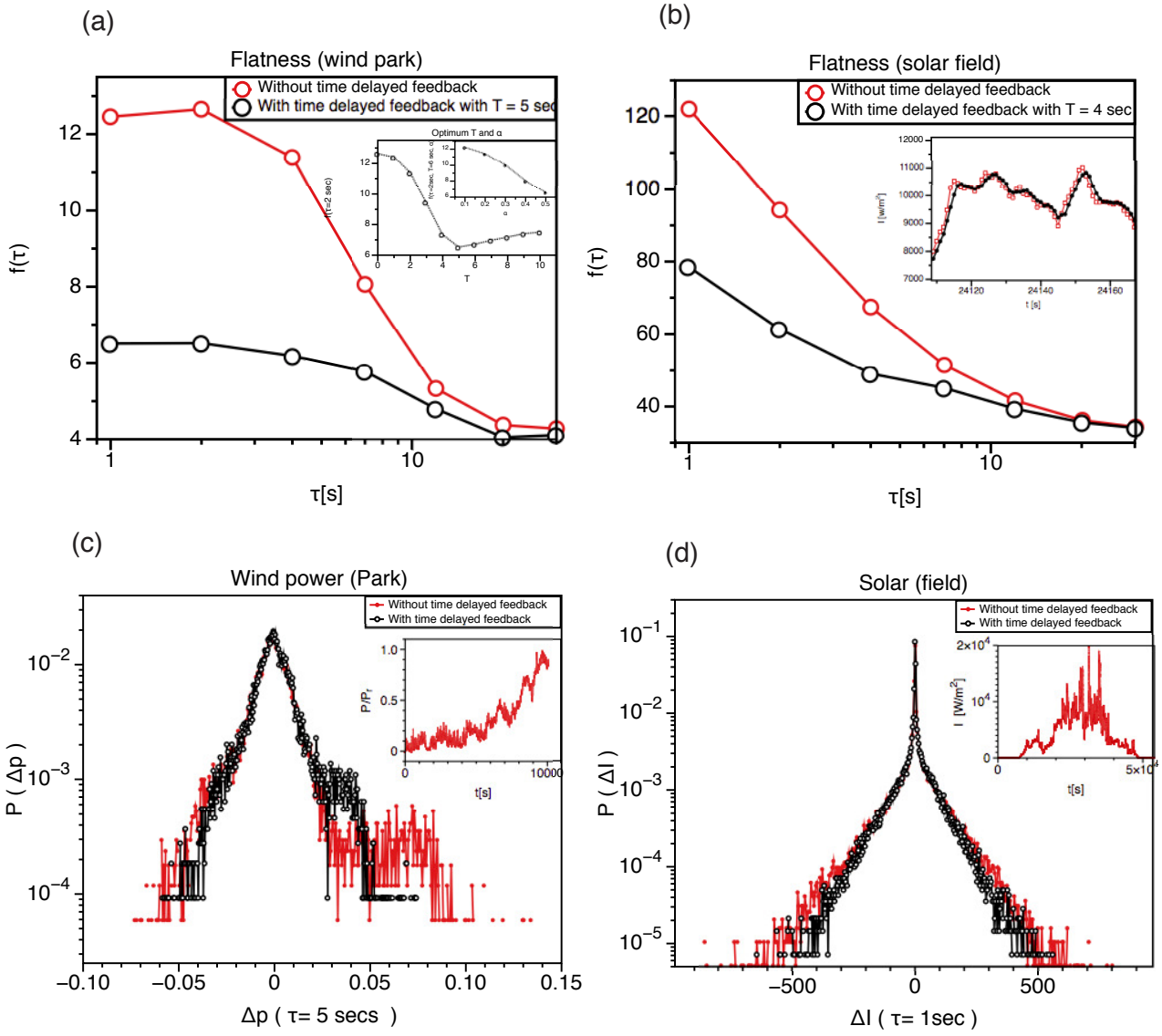

FIG. 9. The results of time delayed feedback method to suppress the short term extreme events of wind farm and solar field. Panels (a-d) show characteristic changes in stochastic dynamics of wind farm and solar field, their flatness (a,b) and probability distribution function of increments (c,d), when applying the time delayed feedback method to control the short time extreme events. The suppressing of extreme events are evident in all panels. In the inset of panel (a) the optimum values of delay lag T and amplification coefficient α in time delayed feedback method with minimizing the flatness in time lag=2 seconds, is shown for a wind farm with 12 turbines. The optimum delay lag is $T = 5$ with $\alpha = 0.5$. In the inset of (b) the power output of solar field is demonstrated and it shows smoother dynamics for the output of the solar field with applying the time delayed feedback method. The results presented in panels (a,c) are derived from 10000 secs of data with sample rate 1Hz, belongs to a time interval that wind farm had strongly intermittent fluctuations, as shown in the inset (c). The data for solar in panel (b) is belongs to a very variable cloudy day in Hawaii (03.03.2011), see inset (d).

to regularly sustain large and rapid changes in speed or direction. These large bursts occur over a wide range of scales in atmospheric flows, from seconds to hours and days [46, 89].

Wind turbines convert such fluctuating wind flow into electrical power. Modern designs are optimized for power efficiency, that implies to react quickly to wind fluctuations. The typical reaction time of wind turbines of $1-5$ MW is estimated as below 20-30 seconds. The wind fluctuations occurring within this reaction time are partly filtered out by the rotor inertia. However, all wind fluctuations that survive longer are converted in a quasi-equilibrium way into mechanical torque and electrical power fluctuations. This effect is not intuitive to anyone observing a rotating wind turbine, as the rotational speed ω is mostly constant. Nevertheless, large fluctuations of mechanical torque N occur, that bring large fluctuations of electrical power $P = N\omega$. Short-time inertia left aside, the power of the wind is a cubic function of the incoming wind speed u, i.e. $P_{wind} \propto u^3$. The electrical power output delivered is $P_{elec} = C_P P_{wind}$. The power coefficient $C_P(u)$ is the efficiency of the turbine, that depends on the wind speed. C_P remains fairly constant and has value $C_P \simeq 0.4$. Large wind gusts bring amplified electrical power gusts, as observed in measurements. The electrical power output of a wind turbine is a very intermittent process, that is often smooth but with occasional large jumps [3, 90].

C. Irradiance to PV Power

In contrast to wind turbines, solar irradiance can be instantaneously (in time scale of μs) transformed to electric power by photovoltaic (PV) cells without any considerable temporal filtering. However, PV power systems are typically made up of multiple PV modules, each in turn consisting of many interconnected PV cells. The larger a PV power system, the more pronounced the possible effect of spatial smoothing thus becomes. Moreover any system's modules will frequently be oriented and tilted in a way to maximize long-term yield by maintaining a preferably high angle of incidence on average. Hence, the farther a PV system is away from the equator, the more will its modules be tilted away from a horizontal position towards the average solar elevation angle.

The entire corresponding process of converting global horizontal irradiance to PV power output is detailed in [91], and its simulation generally begins with calculating the incoming radiant flux density on the PV modules' plane. This is typically done by means of a diffuse model that splits global horizontal irradiance into direct and diffuse fractions, followed by the application of a tilt model that separately converts these two fractions of irradiance to the tilted plane of the PV modules. Subsequently a PV simulation model and an inverter model are used to simulate the PV system performance, thereby accounting for the temperature-dependent efficiency of PV modules and other system characteristics. Thus using global horizontal irradiance as a proxy to analyse the characteristics of PV power feed-in does not necessarily capture all aspects of real PV power production. However, solar irradiance is still the dominating quantity in the process of PV power generation, especially with regards to the characteristics of cloud-induced short-term fluctuations.

When considering typical residential roof-top PV systems, which are relatively small in size but widespread in deployment, and for which appropriate power feed-in data with high spatio-temporal resolution is not readily available, global horizontal irradiance is thus an adequate substitute for the analysis of short-term intermittency. For locations between the Tropic of Cancer and the Tropic of Capricorn, such as Hawaii, this is even more so, because the sun frequently reaches zenith around noon, and PV modules with optimal tilt are expected to be oriented in an almost horizontal fashion. Hence global horizontal irradiance will be almost identical with the solar irradiance on a PV module's plane and an unverifiable simulation-based differentiation of direct and diffuse fractions becomes dispensable. Any discontinuity in solar irradiance, such as jumps in the intensity, would therefore appear immediately in the power output of a small PV system.

D. Germany Irradiance Data

Between May 1992 and March 1994, an observational network consisting of 8 small ($0.242 \times 0.556 m^2$ each) photovoltaic (PV) modules and spanning an area of about $250 \times 250 m^2$ was operated on a platform roof of the University of Oldenburg, Germany (53.152° N, 8.164° E). The system was configured to record fluctuations in mean effective horizontal solar irradiance with a temporal resolution of 1 Hz [92]. The former raw values of the modules' short circuit current measurements are revived from the data archive for this study. First and foremost, the short circuit current of a PV module is proportional to the incident effective solar radiation, but to a lesser extent it also depends on the module temperature, the spectral distribution of incident light, and the angle of incidence accounting for varying optical losses.

For these reasons, deriving precise absolute values of irradiance with high accuracy from the dataset is a nontrivial task that cannot be belatedly performed. Nevertheless, incident effective radiation is the only one of the above

mentioned quantities that fluctuates significantly on short time scales in the range of seconds, while module temperature, spectral distribution of radiation, and angle of incidence depend on comparably slowly changing external circumstances, like ambient temperature, mean wind speed, composition of the atmosphere, and solar elevation angle. By enforcedly neglecting these environmental variables and choosing a constant average calibration factor to calculate effective solar radiation from short circuit current, the relative magnitude of short-term (seconds) fluctuations remains correct, while accuracy on absolute values from day to day goes down.

Based on these constraints and a resulting mean calibration factor c, the raw values of short circuit radiation I_{SC} from the data archive are converted to effective horizontal radiation $G = c * I_{SC}$ and subjected to thorough quality checks to ensure plausible characteristics of all sensors. Any data with dubious characteristics are flagged in the process and removed from the dataset for this study, thereby leaving a total of about 16 million simultaneous measurements of 1 Hz resolution from eight PV modules spread across 398 days as base data for subsequent analyses.

E. Hawaii Irradiance Data

The United States' National Renewable Energy Laboratory (NREL) performed a one-year measurement campaign at Kalaeloa Airport (21.312° N, -158.084° W), Hawaii, USA, from March 2010 until March 2011 using 19 LI-COR LI-200 pyranometers to measure effective solar radiation on horizontal and inclined surfaces with a 1 Hz temporal resolution. Two of the instruments were titled with a 45 degree orientation, while the other 17 were horizontally mounted and scattered across an area of about $750 \times 750m^2$. From this publicly available data pool, the subset of effective horizontal solar radiation was selected, processed and checked to yield about 20 million synchronised values of 1 Hz temporal resolution measured by the aforementioned 17 pyranometers on 378 days.

F. BSRN irradiance data from Algeria (Sahara) and Spain

The Baseline Surface Radiation Network (BSRN) measures solar and atmospheric radiation with instruments of the highest available accuracy and with high temporal resolution (1 to 3 minutes) in different regions of the world (Ohmura et al, 1998 and McArthur, 2005). Multi-year timeseries of global horizontal irradiance were available for one station in northern Spain (1.3 million values recorded between July 2009 and February 2013) and one station in Algeria (3.7 million values recorded between March 2000 and December 2013). The station in Spain is situated in an urban environment in a mountain valley (42.816° N, −1.601° W), while the station in Algeria is surrounded by rock and desert (22.790° N, 5.529° E).

G. Clear-Sky Index Calculation

As changes in effective horizontal solar irradiance are not only the result of stochastic fluctuations but are also governed by deterministic processes, a "detrended" version of irradiance is desired that only exhibits stochastic changes. The dominating deterministic process influencing effective solar radiation is the apparent movement of the sun from earth that accounts for both diurnal and annual variations of the available solar energy on the surface [37]. Thus, by calculating either the extraterrestrial solar irradiance G_{extra} (i.e. irradiance on earth if there were no atmosphere) or the clear-sky irradiance G_{clear} (i.e. irradiance on earth with cloud-free atmosphere) for a location, the instantaneous effective solar irradiance G may be converted to clearness index $k = G/G_{extra}$ or clear-sky index $Z = G/G_{clear}$ respectively. While the extraterrestrial solar irradiance G_{extra} depends only on astronomical relationships, a calculation of clear-sky irradiance G_{clear} also needs to include parameters of atmospheric conditions, such as air composition and turbidity.

For this study, the clear-sky model presented in [93] is used to compute clear-sky irradiance time series for both Germany and Hawaii. In order to ensure conservative results, only data associated with solar elevation angles $\alpha > 10°$ are processed in the clear-sky index calculation. Otherwise, the relatively low effective solar irradiance values occurring after sunrise and before sunset, coupled with path prolongation and corresponding higher uncertainties in radiative transfer calculations at these times, can result in unrealistic clear-sky index values [94]. Consequently, two sets of purely stochastic time series of clear-sky index are derived from the original measurements in Germany and Hawaii. They are independent of the time of day and the time of the year, and comprise around 12 million data for the former and 14 million values for the latter location.

H. Intermittency and increment statistics

Intermittency is a key concept in stochastic processes, which has been born in characterisation of the hydrodynamic turbulence and is associated with the occurrence of bursts of intense motion within more quiescent fluid flow [40]. It leads to strong deviations from Gaussian statistics of fluctuations at short time and length scales [41, 42, 43]. In addition to the studies of hydrodynamic turbulence [41], intermittency has been also observed in systems involving transport by a turbulent flow [44], in granular systems [95], in magneto-hydrodynamic turbulence in geophysics [96], in the solar wind [97], in stock price fluctuations [98], in seismic series [99], and in plasma turbulence [100, 101].

To quantify the intermittency Frisch and Parisi [102] introduced a multi-scale description of fluctuation quantity $x(t)$ using the increment statistics, i. e. $\Delta x(\tau) = x(t+\tau)x(t)$. To characterize the non-linearity of fluctuations they considered the order-p structure functions $S_p(\tau) = \langle |\Delta x|^p \rangle$ and studied their power-law behaviour at short time lag τ, $S_p \sim \tau^{\xi_p}$. The exponents ξ_p scale linearly with p when the fluctuations are homogeneous at all scales. On the contrary, the non-linear dependence of ξ_p on p corresponds to nonhomogeneous fluctuations, and it is a hallmark of intermittency [40, 102].

Also in parallel relevant information to characterize intermittency can be also obtained from the analysis of the distribution of increments [40]. With respect to strong non-Gaussian statistics wind and solar power in lag τ existence of both large increments (with diffusive power fluctuations) and jumps could have similar impact. Disentangling of the effects caused by the diffusive behavior from the effects of jumps is one of main problem in detailed understanding of stochastic dynamics of complex systems. The effective potential and determination of its attractors and jump (flickering) rates between them, enables us to understand and characterize the short-term fluctuations of wind and solar power. As shown in Fig. 2c, with increasing the fields size the jumpy of flickering behavior of cumulative power is suppressed and cumulative power output has a diffusive characteristics.

I. Effective potential

We would like to determine the effective potential of solar irradiance and wind power time series. The time series are rated power $P(t) \equiv P(t)/P_r$ for wind and clear sky index. We assume that their dynamics can be written as [50, 52]:

$$\frac{dP(t)}{dt} = D^{(1)}(P) + \sqrt{D^{(2)}(P)} \cdot \Gamma(t) \tag{2}$$

where the coefficients $D^{(n)}(P)$ can be estimated in a non-parametric way from measurement data as Kramers-Moyal coefficients:

$$D^{(n)}(P) = lim_{\tau \to 0} \frac{1}{n!\tau} \langle [P(t+\tau) - P(t)]^n | P(t) = P \rangle. \tag{3}$$

The drift and diffusion functions are defined as $D^{(1)}(P)$ and $D^{(2)}(P)$, respectively. The random function Γ in Eq. (2), is a zero-mean Gaussian uncorrelated noise with variance 2 [52]. Equation (2) means that the stochastic behaviour of the power $P(t)$ is disentangled into a deterministic drift $D^{(1)}(P)$ plus some random fluctuations $\sqrt{D^{(2)}(P)}\Gamma$ where the amplitude of the noise is controlled by the local diffusion coefficient $D^{(2)}(P)$. There are two origins for the non-linearity in the stochastic equation (2): non-linearity in the drift term $D^{(1)}(P)$ or respectively in the multiplicative term $D^{(2)}(P)$. We can define a local-potential $U(P) = -\int_{-\infty}^{P} D^{(1)}(P')dP'$, which gives the local information that belongs to the additive part of dynamics. The effective-potential is defined as $U_{eff}(P) = \ln D^{(2)}(P) - \int_{-\infty}^{P} [D^{(1)}(P')/D^{(2)}(P')]dP'$, which depends on both additive and multiplicative terms [50, 52]. Here $D^{(2)}(P)$ plays the role of a local temperature in generalised Brownian-type dynamics. The effective potential provides the probability density function of time series as, $Prob(P) \sim \exp(-U_{eff}(P))$. The structure (number of minima, etc.) of the two potentials $U(P)$ and $U_{eff}(P)$ can be different, in general.

[1] A. Schavan, Germany's Energy Research Plan, Science **330**, 295 (2010).
[2] M. Amin, Energy: The smart-grid solution, Nature **499**, 145 (2013).
[3] P. Milan, M. Wächter, and J. Peinke, Turbulent Character of Wind Energy, Phys. Rev. Lett. **110**, 138701 (2013) .
[4] E. Hau "Windturbines, Fundamentals, Technologies, Applications, Economics", (Springer, Berlin,2000).

[5] W. Winter European wind integration study (EWIS)-Towards a successful integration of wind power into european electricity grids. Technical report, ENTSO-E (2007).

[6] ENTSO-E, System adequacy forecast 2010-2025. Technical report (2010).

[7] A. Nieße, M. Tröschel, M. Sonnenschein, Designing dependable and sustainable Smart GridsHow to apply Algorithm Engineering to distributed control in power systems, Environmental Modelling & Software **56**, 37 (2014).

[8] R. Baldick *et al.*, Initial review of methods for cascading failure analysis in electric power transmission systems, IEEE PES CAMS task force on understanding, prediction, mitigation and restoration of cascading failures, IEEE Power Engineering Society General Meeting, 10142341, 1, (2008).

[9] B. A. Carreras, V. E. Lynch, M. L. Sachtjen, I. Dobson, and D. E. Newman, Modeling Blackout Dynamics in Power Transmission Networks, Hawaii International Conference on System Sciences, January 3-6, Maui, Hawaii, (2001).

[10] I. Dobson, B. A. Carreras, V. E. Lynch, and D. E. Newman, Complex systems analysis of series of blackouts: cascading failure, critical points, and self organization, *Chaos* **17** (2), 026103 (2007).

[11] G. Nicolis and I. Prigogine, *Exploring Complexity* (W. H. Freeman, San Francisco, 1989).

[12] B. A. Carreras, D. E. Newman, I. Dobson, and A. B. Poole, Evidence for self-organized criticality in a time series of electric power system blackouts, *IEEE Trans. Circuits & Systems I* **51**, 1733 (2004).

[13] M. Rohden, A. Sorge, M. Timme and D. Witthaut, Self-Organized Synchronization in Decentralized Power Grids, Phys. Rev. Lett. **109**, 064101, (2012).

[14] D. Witthaut and M. Timme. Braess's paradox in oscillator networks, desynchronization and power outage, New J. Phys. **14**, 083036, (2012).

[15] M. Chertkov, M. Stepanov, F. Pan, and R. Baldick, Exact and Efficient Algorithm to Discover Extreme Stochastic Events in Wind Generation over Transmission Power Grids, http://arxiv.org/1104.0183, (2011) .

[16] J. Heitzig, N. Fujiwara, K. Aihara and J. Kurths, Interdisciplinary challenges in the study of power grid resilience and stability and their relation to extreme weather events, Eur. Phys. J. Special Topics 223(12), 2281, (2014).

[17] C. Kamath, Understanding wind ramp events through analysis of historical data," in Transmission and Distribution Conference and Exposition, IEEE PES,1, (2010).

[18] S. Tunc, Enhancement of solar ultraviolet surface irradiance under partial cloudy conditions, Graduation research, at KNMI, De Bilt, The Netherlands, (1999).

[19] N. H. Schade et al., Enhanced solar effective irradiance during cloudy sky conditions, MeteorologischeZeitschrift **16**, 295, (2007) .

[20] G. Thuillier, J.-M Perrin, P. Keckhut, and F. Huppert, Local enhanced solar irradiance on the ground generated by cirrus: measurements and interpretation, Appl. Remote Sens. **7**, 073543, (2013).

[21] J. Apt, The spectrum of power from wind turbines," Journal of Power Sources, vol. **169**, 369, (2007) .

[22] A. E. Curtright and J. Apt, The Character of Power Output from Utility-Scale Photovoltaic Systems, Prog. Photovolt: Res. Appl. **16** 241, (2008).

[23] W. Katzenstein, E. Fertig, J. Apt, The variability of interconnected wind plants, Energy Policy **38** 4400, (2010).

[24] C. Lueken, G. E. Cohen, J. Apt, Costs of Solar and Wind Power Variability for Reducing CO2 Emissions, Environ. Sci. Technol. **46**, 9761, (2012).

[25] M. Reza Rahimi Tabar, M. Anvari, G. Lohmann, D. Heinemann, M. Wächter, P. Milan, E. Lorenz, and J. Peinke, Kolmogorov spectrum of renewable wind and solar power fluctuations, Eur. Phys. J. Special Topics 223(12), 2637, (2014).

[26] G. Lohmann, M Reza Rahimi Tabar, P. Milan, M. Anvari, M. Wächter, E. Lorenz, D. Heinemann and J. Peinke, Flickering Events in Wind and Solar Power, Proceedings of the 28th Conference on Environmental Informatics - Informatics for Environmental Protection, Sustainable Development and Risk Management, EnviroInfo 2014 - ICT for Energy Efficiency 723, (2014).

[27] A. Woyte, V. V. Thong, R. Belmans, and J. Nijs, Voltage fluctuations on distribution level introduced by photovoltaic systems, IEEE Transactions on Energy Conversion, **21**, 202, (2006).

[28] A. Woyte, R. Belmans, and J. Nijs, Fluctuations in instantaneous clearness index: Analysis and statistics, Solar Energy **81**, 195, (2007).

[29] A. Woyte, R. Belmans, and J. Nijs, Localized Spectral Analysis of Fluctuating Power Generation from Solar Energy Systems, EURASIP Journal on Advances in Signal Processing, 80919, (2007).

[30] J. Marcos, L. Marroyo, E. Lorenzo, D. Alvira and E. Izco, Power output fluctuations in large scale pv plants: One year observations with one second resolution and a derived analytic model, Progress in Photovoltaics: Research and Applications **19**, 218, (2011).

[31] A. Peled and J. Appelbaum, Evaluation of solar radiation properties by statistical tools and wavelet analysis, Renewable energy **59**, 30, (2013).

[32] T. E. Hoff and R. Perez, Quantifying PV power output variability, Solar Energy **84**, 1782, (2010) .

[33] M. Lave and J. Kleissl, Solar variability of four sites across the state of Colorado," Renewable Energy, **35** 2867, (2010).

[34] J. Marcos, L. Marroyo, E. Lorenzo, D. Alvira, and E. Izco, From irradiance to output power fluctuations: the PV plant as a low pass filter, Progress in Photovoltaics: Research and Applications, **19**, 505, (2011).

[35] T. E. Hoff and R. Perez, Modeling PV fleet output variability, Solar Energy **86** 2177, (2012).

[36] J. M. Vindel and J. Polo, Intermittency and variability of daily solar irradiation, Atmospheric Research **143** 313, (2014).

[37] M. Lave, J. Kleissl and E. Arias-Castro, High-frequency irradiance fluctuations and geographic smoothing, Solar Energy **86** 2190, (2012).

[38] M. Lave, J. Kleissl, Cloud speed impact on solar variability scaling - Application to the wavelet variability model, Solar Energy **91** 11, (2013).

[39] M. Lave, J. Kleissl and J. Stein, A Wavelet-based Variability Model (WVM) for Solar PV Power Plants, IEEE Transactions on Sustainable Energy, **4**, 501, (2013).
[40] U. Frisch, Turbulence: The Legacy of A. N. Kolmogorov, Cambridge University Press, (1996).
[41] B. Castaing, Y. Gagne and E. Hopfinger, Velocity probability density functions of high Reynolds number turbulence, Phys. D Nonlinear Phenom. **46** (2), 177, (1990).
[42] L. Chevillard, C. Meneveau, Lagrangian Dynamics and Statistical Geometric Structure of Turbulence, Phys. Rev. Lett., **97** 174501, (2006).
[43] K. R. Sreenivasan, Fluid turbulence, Reviews of Modern Physics **71** S383, (1999).
[44] G. Falkovich, K. Gawedzki, and M. Vergassola, Particles and fields in fluid turbulence, Rev. Mod. Phys. **73** 913, (2001).
[45] O. Kamps, Characterizing the fluctuations of wind power production by multi-time statistics, in Wind Energy - Impact of Turbulence, Eds: M. H́olling, J. Peinke, S. Ivanell, (Springer, Berlin, Heidelberg, 2014).
[46] R. Baïle and J. -F. Muzy, Spatial intermittency of surface layer wind fluctuations at mesoscale range, *Phys. Rev. Lett.* **105**, 254501, (2010).
[47] R. Wood and P.R. Field, The distribution of cloud horizontal sizes, *J. Climate* **24**, 4800, (2011).
[48] M. Scheffer, et al. Anticipating Critical Transitions, Science **338**, 344, (2012).
[49] L. Dai, D. Vorselen, K. S. Korolev and J. Gore, Generic indicators for loss of resilience before a tipping point leading to population collapse, Science **336**, 1175, (2012).
[50] M. Hirota, M. Holmgren, E. H.Van Nes, M. Scheffer, Global resilience of tropical forest and savanna to critical transitions, Science **334**, 232, (2011).
[51] H. Haken, Advanced Synergetics, Instability hierarchies and self-organizing systems and devices, (Springer, Berlin, 1983).
[52] R. Friedrich, J. Peinke , M. Sahimi and M. R. Rahimi Tabar, Approaching complexity by stochastic methods: From biological systems to turbulence, Phys. Rep. **506**, 87, (2011).
[53] F. Blaabjerg, Z. Chen and S. B. Kjaer, Power electronics as efficient interface in dispersed power generation systems, *Power Electronics, IEEE Transactions on* **19** 1184, (2004).
[54] J. Marcos O. Storkél, L. Marroyo, M. Garcia and E. Lorenzo, Storage requirements for PV power ramp-rate control, Solar Energy **99** 28, (2014).
[55] J. Marcos, I. de la Parra, M. García and L. Marroyo, Control Strategies to Smooth Short-Term Power Fluctuations in Large Photovoltaic Plants Using Battery Storage Systems, Energies **7**, 6593, (2014).
[56] A. Keyhani and M. Marwali (eds.) Smart Power Grids 2011 (Springer, Berlin, 2012).
[57] X. Fang,S. Misra, G. Xue, and D. Yang, Smart grid-The new and improved power grid: A survey, IEEE, **14** (4), 944, (2012).
[58] R. Perez, P. Ineichen, R. Seals, J. Michalsky and R. Stewart, Modeling daylight availability and irradiance components from direct and global irradiance, *Solar energy* **44**, 271, (1990).
[59] E. Lorenz, J. Hurka, D. Heinemann and H. G. Beyer, Irradiance Forecasting for the Power Prediction of Grid-Connected Photovoltaic Systems, *IEEE Journal of selected topics in applied earth observations and remote sensing*, **2**, 2, (2009).
[60] E. Lorenz, J. Kühnert and D. Heinemann "Overview on Irradiance and Photovoltaic Power Prediction", in Weather Matters for Energy, Springer, Editors: A. Troccoli, L. Dubus, S. E. Haupt, (2014).
[61] M. Lipperheide, J. L. Bosch and J. Kleissl, Embedded nowcasting method using cloud speed persistence for a photovoltaic power plant, Solar Energy **112** 232, (2015).
[62] K. Lappalainen and S. Valkealahti, Recognition and modelling of irradiance transitions caused by moving clouds, Solar Energy **112** 55, (2015).
[63] W. Just, T. Bernard, M. Ostheimer, E. Reibold, and H. Benner, Mechanism of Time-Delayed Feedback Control, *Phys. Rev. Lett.* **78**, 203, (1997).
[64] M. G. Rosenblum and A. S. Pikovsky, Controlling synchronization in an ensemble of globally coupled oscillators, *Phys. Rev. Lett.* **92**, 114102, (2004).
[65] S. Koch, K. Heussen, A. Ulbig, G. Andersson, Unified system-level modeling of intermittent renewables and energy storage in power system operation, Systems Journal, IEEE, PP(99), 1, (2011).
[66] N. Kakimoto, H. Satoh, S. Takayama, K. Nakamura, Ramp-rate control of photovoltaic generator with electric double-layer capacitor, IEEE Trans. Energy Convers. **24**, 465, (2009).
[67] X. Li, D. Hui, X. Lai, Battery energy storage station (BESS)-based smoothing control of photovoltaic (PV) and wind power generation fluctuations. IEEE Trans. Sustain. Energy **4**, 464, (2013).
[68] M. Alam, K. Muttaqi, D. Sutanto, A novel approach for ramp-rate control of solar PV using energy storage to mitigate output fluctuations caused by cloud passing. IEEE Trans. Energy Convers. **29**, 507, (2014).
[69] N. Kakimoto, H. Satoh, S. Takayama and K. Nakamura , Ramp-rate control of photovoltaic generator with electric double-layer capacitor. IEEE Trans. Energy Convers. **24**, 465, (2009).
[70] L. N. Khanh, J.-J. Seo, Y.-S. Kim and D.-J. Won, Power-management strategies for a grid-connected PV-FC hybrid system. IEEE Trans. Power Deliv. **25**, 1874, (2010).
[71] R. Yan and T.K. Saha Power ramp rate control for grid connected photovoltaic system. In Proceedings of the 2010 IPEC Conference, Singapore, 2729,83, (2010).
[72] L. Wang and Y.-H. Lin, Random fluctuations on dynamic stability of a grid-connected photovoltaic array. In Proceedings of the 2001 IEEE Power Engineering Society Winter Meeting, Columbus, OH, USA; Volume 3, pp. 985, (2001).
[73] X. Li, D. Hui and X. Lai, Battery energy storage station (BESS)-based smoothing control of photovoltaic (PV) and wind power generation fluctuations. IEEE Trans. Sustain. Energy **4,** 464, (2013).

[74] M. Alam, K. Muttaqi and D. Sutanto, A novel approach for ramp-rate control of solar PV using energy storage to mitigate output fluctuations caused by cloud passing. IEEE Trans. Energy Convers. **29**, 507; Energies **7** 6618, (2014) .

[75] M. Datta, T. Senjyu, A. Yona, T. Funabashi and C.-H Kim, Photovoltaic output power fluctuations smoothing methods for single and multiple PV generators. Curr. Appl. Phys. **10**, S265, (2010).

[76] H.-R. Seo, G.-H. Kim, S.-Y. Kim, N. Kim, H.-G. Lee, C. Hwang, M. Park and I.-K. Yu, Power quality control strategy for grid-connected renewable energy sources using PV array and supercapacitor. In Proceedings of the 2010 International Conference on Electrical Machines and Systems (ICEMS), Incheon, Korea, 437, (2010).

[77] P. Chanhom, S. Sirisukprasert and N. Hatti, A new mitigation strategy for photovoltaic power fluctuation using the hierarchical simple moving average. In Proceedings of the 2013 IEEE International Workshop on Intelligent Energy Systems (IWIES), Vienna, Austria, 28, (2013).

[78] X. Han, F. Chen, X. Cui, Y. Li and X. Li, A power smoothing control strategy and optimized allocation of battery capacity based on hybrid storage energy technology. Energies **5**, 1593, (2012).

[79] C, Nicolis, V. Balakrishnan and G. Nicolis, Extreme Events in Deterministic Dynamical Systems, *Phys. Rev. Lett.* **97**, 210602, (2006).

[80] *Extreme Events in Nature and Society*, Edited by: S. Albeverio, V. Jentsch & H. Kantz (Springer, Berlin, 2006).

[81] H. Farhangi, The Path of the Smart Grid, IEEE Power and Energy Magazine **8**, 18, (2010).

[82] H. Kanchev, Di Lu; F. Colas, V. Lazarov and B. Francois, Energy Management and Operational Planning of a Microgrid With a PV-Based Active Generator for Smart Grid Applications, IEEE Transactions on Industrial Electronics **58**, 4583, (2011).

[83] H. Haken *Synergetics: Introduction and Advanced Topics* (Springer, Berlin, 2004).

[84] S. V. Buldyrev, R. Parshani, G. Paul, H. E. Stanley and S. Havlin, Catastrophic cascade of failures in interdependent networks, Nature **464**, 1025, (2010).

[85] P. J. Menck, J. Heitzig, N. Marwan and J. Kurths, How basin stability complements the linear-stability paradigm, Nature Physics **9**, 89, (2013).

[86] P. Menck, J. Heitzig, J. Kurths, H.J. Schellnhuber, How dead ends undermine power grid stability, Nat. Commun. **5**, 3969, (2014) .

[87] T. Dewenter and A. K. Hartmann, Large-deviation properties of resilience of power grids, arXiv:1411.5233, (2014).

[88] R. Pereza, T. Hoff, J. Dise, D. Chalmers and S. Kivalov, The cost of mitigating short-term PV output variability, Energy Procedia **57** 755, (2014).

[89] F. Böttcher, St. Barth, and J. Peinke, Small and Large Scale Fluctuations in Atmospheric Wind Speeds, *Stochastic Environmental Research and Risk Assessment* (SERRA) **21**, 299, (2007) .

[90] M. Wächter, et al., Wind energy and the turbulent nature of the atmospheric boundary layer, *Journal of Turbulence* **13**,1, (2012).

[91] E. Lorenz and D. Heinemann, Prediction of solar irradiance and photovoltaic power, in Comprehensive Renewable Energy, A. Sayigh, Ed. Oxford: Elsevier, 2012, pp. 239-292. [Online]. Available: http://www.sciencedirect.com/science/article/pii/B9780080878720001141.

[92] H. G. Beyer, A. Hammer, J. Luther, J. Poplawska, K. Stolzenburg and P. Wieting, Analysis and synthesis of cloud pattern for radiation field studies, *Solar energy* **52**, 379, (1994).

[93] M. Fontoynont, et al. "Satellight: a WWW server which provides high quality daylight and solar radiation data for Western and Central Europe." Proceedings of the 9th Conference on Satellite Meteorology and Oceanography. No. 2, (1998).

[94] A. Woyte, R. Belmans and J. Nijs, Fluctuations in instantaneous clearness index: Analysis and statistics, *Solar Energy* **81**, 195, (2007).

[95] F. Radjai and S. Roux, Turbulentlike Fluctuations in Quasistatic Flow of Granular Media, Phys. Rev. Lett., **89** 5, (2002).

[96] P. D. Michelis and G. Consolini, Time intermittency and spectral features of the geomagnetic field, Ann. Geophys., **47** 1713, (2004).

[97] O. Alexandrova , V. Carbone, P. Veltri and L. Sorriso-Valvo, Solar wind Cluster observations: Turbulent spectrum and role of Hall effect, Planet. Space Sci., **55** 2224, (2007).

[98] K. Kiyono, Z. R. Struzik, and Y. Yamamoto, Criticality and Phase Transition in Stock-Price Fluctuations, Phys. Rev. Lett., **96** 1, (2006).

[99] P. Manshour, S. Saberi, M. Sahimi, J. Peinke, Amalio F. Pacheco, M. Reza Rahimi Tabar, Turbulencelike Behavior of Seismic Time Series, Phys. Rev. Lett., **102** 14101, (2009).

[100] B. Ph. van Milligen, C. Hidalgo, and E. Sánchez, Nonlinear phenomena and intermittency in plasma turbulence, Phys. Rev. Lett., **74** 395, (1995) .

[101] J. A. Mier, R. Sánchez, L. García, B. A. Carreras, and D. E. Newman, Characterization of Nondiffusive Transport in Plasma Turbulence via a Novel Lagrangian Method, Phys. Rev. Lett., **101** 1, (2008).

[102] U. Frisch and G. Parisi, Turbulence and Predictability in Geophysical Fluid Dynamics and Climate Dynamics, in B. R. Ghil M. and P. G., eds, Proc. Enrico Fermi Varenna Phys. Sch. LXXXVIII", North-Holland, Amsterdam, p. 84, (1985).